Monthly Notices
of the
ROYAL ASTRONOMICAL SOCIETY

Mon. Not. R. Astron. Soc. **426,** 3201–3210 (2012) doi:10.1111/j.1365-2966.2012.21941.x

The evolutionary connection between QSOs and SMGs: molecular gas in far-infrared luminous QSOs at $z \sim 2.5$

J. M. Simpson,[1⋆] Ian Smail,[1] A. M. Swinbank,[1] D. M. Alexander,[1] R. Auld,[2] M. Baes,[3] D. G. Bonfield,[4] D. L. Clements,[5] A. Cooray,[6] K. E. K. Coppin,[7] A. L. R. Danielson,[1] A. Dariush,[2,5] L. Dunne,[8] G. de Zotti,[9,10] C. M. Harrison,[1] R. Hopwood,[5] C. Hoyos,[11] E. Ibar,[12] R. J. Ivison,[12,13] M. J. Jarvis,[4,14] A. Lapi,[10,15] S. J. Maddox,[8] M. J. Page,[16] D. A. Riechers,[17] E. Valiante[2] and P. P. van der Werf[18]

[1]*Institute for Computational Cosmology, Department of Physics, Durham University, South Road, Durham DH1 3LE*
[2]*School of Physics and Astronomy, Cardiff University, Queen's Buildings, The Parade, Cardiff CF24 3AA*
[3]*Sterrenkundig Observatorium, Universiteit Gent, Krijgslaan 281 S9, B-9000 Gent, Belgium*
[4]*Centre for Astrophysics Research, Science & Technology Research Institute, University of Hertfordshire, Hatfield AL10 9AB*
[5]*Astrophysics Group, Blackett Lab, Imperial College, Prince Consort Road, London SW7 2AZ*
[6]*Department of Physics and Astronomy, University of California, Irvine, CA 92697, USA*
[7]*Department of Physics, McGill University, 3600 Rue University, Montréal, QC H3A 2T8, Canada*
[8]*Department of Physics and Astronomy, University of Canterbury, Private Bag 4800, Christchurch 8140, New Zealand*
[9]*INAF – Osservatorio Astronomico di Padova, Vicolo Osservatorio 5, I-35122 Padova, Italy*
[10]*SISSA, Via Bonomea 265, I-34136 Trieste, Italy*
[11]*School of Physics and Astronomy, University of Nottingham, University Park, Nottingham NG7 2RD*
[12]*UK Astronomy Technology Centre, Royal Observatory, Blackford Hill, Edinburgh EH9 3HJ*
[13]*Institute for Astronomy, University of Edinburgh, Blackford Hill, Edinburgh EH9 3HJ*
[14]*Physics Department, University of the Western Cape, Cape Town 7535, South Africa*
[15]*Dipartimento di Fisica, Università Tor Vergata, Via della Ricerca Scientifica 1, 00133 Roma, Italy*
[16]*Mullard Space Science Laboratory, University College London, Holmbury St Mary, Dorking, Surrey RH5 6NT*
[17]*California Institute of Technology, MC 249-17, 1200 East California Boulevard, Pasadena, CA 91125, USA*
[18]*Leiden Observatory, Leiden University, PO Box 9513, 2300 RA Leiden, the Netherlands*

Accepted 2012 August 15. Received 2012 August 14; in original form 2012 June 20

ABSTRACT

We present Institut de Radioastronomie Millimétrique Plateau de Bure Interferometer observations of the ^{12}CO (3–2) emission from two far-infrared luminous QSOs at $z \sim 2.5$ selected from the *Herschel*-Astrophysical Tetrahertz Large Area Survey. These far-infrared bright QSOs were selected to have supermassive black holes (SMBHs) with masses similar to those thought to reside in submillimetre galaxies (SMGs) at $z \sim 2.5$, making them ideal candidates as systems in the potential transition from an ultraluminous infrared galaxy phase to a submillimetre faint, unobscured, QSO. We detect ^{12}CO (3–2) emission from both QSOs and we compare their baryonic, dynamical and SMBH masses to those of SMGs at the same epoch. We find that these far-infrared bright QSOs have similar dynamical but lower gas masses than SMGs. We combine our results with literature values and find that at a fixed $L_{\rm FIR}$, far-infrared bright QSOs have $\sim$50 $\pm$ 30 per cent less warm/dense gas than SMGs. Taken together with previous results, which show that QSOs lack the extended, cool reservoir of gas seen in SMGs, this suggests that far-infrared bright QSOs are at a different evolutionary stage. This is consistent with the hypothesis that far-infrared bright QSOs represent a short ($\sim$1 Myr) but ubiquitous phase in the transformation of dust-obscured, gas-rich, starburst-dominated SMGs into unobscured, gas-poor, QSOs.

⋆E-mail: j.m.simpson@dur.ac.uk

Key words: galaxies: evolution – galaxies: formation – quasars: emission lines – quasars: individual: J0908−0034 – quasars: individual: J0911+0027.

1 INTRODUCTION

An evolutionary link between local ultraluminous infrared galaxies [ULIRGs, with far-infrared (FIR) luminosities of $L_{\rm FIR} \geq 10^{12}\,{\rm L}_{\odot}$] and quasi-stellar objects (QSOs[1]) was first suggested by Sanders et al. (1988) and considerable effort has been expended to test this connection in the local Universe (e.g. Tacconi et al. 2002; Veilleux et al. 2009). This hypothesis has been strengthened by the discovery of a relation between the mass of supermassive black holes (SMBHs) and the mass of their host spheroids (e.g. Magorrian et al. 1998; Ferrarese & Merritt 2000; Gebhardt et al. 2000), which suggests a physical connection between the growth of spheroids and their SMBHs. As shown by theoretical simulations, such a link can be formed through the suppression of star formation in a host galaxy by winds and outflows from an active galactic nucleus (AGN) at its centre (Di Matteo, Springel & Hernquist 2005; Hopkins et al. 2005).

Both the ULIRG and QSO populations evolve very rapidly with redshift, and although subject to selection biases, intriguingly both populations appear to reach a broad peak in their activity at $z \sim 2.5$ (Shaver 1988; Chapman et al. 2005; Wardlow et al. 2011). The high-redshift ULIRGs, which are typically bright at submillimetre (submm) wavelengths, and hence are called submm galaxies (SMGs), are thought to represent the formation of massive stellar systems through an intense burst of star formation in the early Universe, potentially triggered by mergers of gas-rich progenitors (Frayer et al. 1998; Blain et al. 2002; Swinbank et al. 2006, 2010; Tacconi et al. 2006, 2008; Engel et al. 2010) or cold accretion flows (Birnboim & Dekel 2003; Dekel et al. 2009).

The similarity in the redshift distribution of the SMGs and QSOs may be indicating that the evolutionary link between these populations, which has been postulated locally, also holds at $z \sim 2$, when both populations were much more numerous and significant in terms of stellar mass assembly. Indeed, recent work on the clustering of $z \sim 2$ QSOs and SMGs has shown that both populations reside in parent haloes of similar mass, $M_{\rm halo} \sim 10^{13}\,{\rm M}_{\odot}$ (Hickox et al. 2012), adding another circumstantial connection between them. Moreover, this characteristic $M_{\rm halo}$ is similar to the mass at which galaxy populations transition from star-forming to passive systems (e.g. Brown et al. 2008; Coil et al. 2008; Hartley et al. 2010), which may be indirect evidence for the influence of QSO feedback on star formation in galaxies (Granato et al. 2001; Lapi et al. 2006). One final circumstantial link between SMGs and QSOs comes from estimates of the masses of SMBHs in SMGs. Due to the dusty nature of SMGs these studies are inherently challenging, yielding results with more scatter than seen for optical quasars. However, they suggest that the SMBH masses are $\sim 10^{8}\,{\rm M}_{\odot}$, significantly lower than seen in comparably massive galaxies at the present day (Alexander et al. 2008). This indicates the need for a subsequent phase of SMBH growth, which could be associated with a QSO phase.

One puzzling issue about the proposed evolutionary connection between high-redshift QSOs and SMGs is that only a small fraction of submm-detected galaxies ($S_{850} \gtrsim 5\,{\rm mJy}$) are identified as optically luminous, $M_B \leq -22$, $z \sim 1$–3 QSOs (∼2 per cent; Chapman et al. 2005; Wardlow et al. 2011), indicating that, if they are related, then the QSO and ULIRG phases do not overlap significantly. Taken together, these various results provide support for an evolutionary link between high-redshift ULIRGs (SMGs) and QSOs, with a fast transition (∼1 Myr) from the star formation dominated SMG phase to the AGN-dominated QSO phase (e.g. Page et al. 2012), where rapid SMBH growth can then subsequently account for the present-day relation between spheroid and SMBH masses. In this scenario, when a QSO *is* detected in the FIR/submm it will be in the transition phase from an SMG to an unobscured QSO, making its physical properties (e.g. gas mass, dynamics, etc.) a powerful probe of the proposed evolutionary cycle (e.g. Page et al. 2004, 2011; Stevens et al. 2005).

In this paper, we present a study with the Institut de Radioastronomie Millimétrique (IRAM) Plateau de Bure Interferometer (PdBI) of the cold molecular gas in two FIR-selected 'transition' candidate QSOs from the *Herschel Space Observatory*[2] (Pilbratt et al. 2010) Astrophysical Tetrahertz Large Area Survey (H-ATLAS; Eales et al. 2010). We detect ^{12}CO (3–2) in both FIR-bright QSOs studied, and compare the gas and kinematic properties of these to other ^{12}CO-detected QSOs and SMGs to relate their evolution. Throughout we adopt cosmological parameters from Spergel et al. (2003) of $\Omega_{\rm m} = 0.27$, $\Omega_{\Lambda} = 0.73$ and $H_0 = 71\,{\rm km\,s^{-1}\,Mpc^{-1}}$.

2 OBSERVATIONS AND DATA REDUCTION

2.1 Sample selection

Our aim is to study the molecular gas and dynamical properties of FIR-bright QSOs to test their evolutionary link to SMGs, for which larger samples are now available (Greve et al. 2005; Bothwell et al. 2012). We focus our study on potential transition (FIR-bright) QSOs at the era when the activity in both the QSO and SMG populations peaked, $z \sim 2.5$. Previous ^{12}CO studies of unlensed FIR- or submm-bright QSOs (Coppin et al. 2008, including data from Beelen et al. 2004) have usually studied the most luminous QSOs, with SMBH masses one to two orders of magnitude larger than those seen in typical SMGs and correspondingly low space densities. Both of these factors make it hard to test an evolutionary link between these QSOs and typical SMGs [studies of lensed QSO samples, Riechers (2011), also suffer from the difficulty of determining the true space densities of the sources being studied]. The limitations of these previous studies arose because of the lack of large samples of FIR/submm-detected QSOs; hence, Coppin et al. (2008) selected a sample of luminous QSOs which were later found to be bright in the submm. However, with the advent of wide-field FIR/submm surveys with *Herschel* we can now select samples of QSOs with redshifts, space densities, FIR luminosities and most critically SMBH masses which are well matched to those of the hypothesized descendents of typical SMGs.

[1] Defined as having $M_B \leq -22$ and one or more broad emission lines with a width $\geq 1000\,{\rm km\,s^{-1}}$.

[2] *Herschel* is an ESA space observatory with science instruments provided by European-led Principal Investigator consortia and with important participation from NASA.

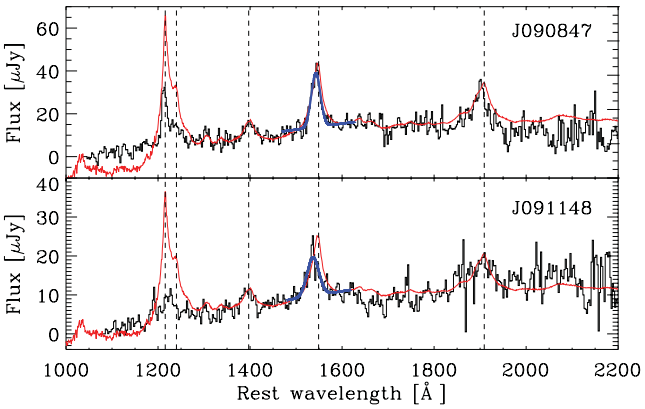

Figure 1. The 2SLAQ UV rest-frame spectra for both QSOs in our sample from Croom et al. (2009), with the 2QZ composite QSO spectrum overlaid (red; Croom et al. 2002). From left to right, dashed lines indicate the rest wavelengths of Lyα, N V, Si IV, C IV and C III] emission. Both QSOs, but especially J0911+0027, have relatively weak Lyα 1215 emission when compared to C IV 1549, suggesting the presence of significant quantities of neutral gas in their vicinity (see also Omont et al. 1996). For each QSO, we estimate the SMBH mass from the FWHM of the C IV 1549 line and the rest-frame 1350-Å luminosity (Vestergaard & Peterson 2006). The FWHM of the C IV line is derived from the best-fitting Gaussian and continuum model (shown in blue), which provides an adequate fit to the emission line in both cases: $\chi^2_r = 1.4$ for J0908−0034 and $\chi^2_r = 1.5$ for J0911+0027. The rest wavelength scale of the plots is based on the systemic redshifts derived from ^{12}CO (3–2) (see Section 3).

For our analysis, we have therefore used the sample of FIR-observed QSOs from Bonfield et al. (2011), which are derived from the survey of the 9 h H-ATLAS field (Eales et al. 2010). Bonfield et al. (2011) extracted FIR fluxes from the *Herschel* Spectral and Photometric Imaging Receiver (SPIRE) 250-, 350- and 500-μm maps (Griffin et al. 2010; Pascale et al. 2011) at the optical position of 372 QSOs from either Sloan Digital Sky Survey (SDSS; Schneider et al. 2010) or the 2dF-SDSS luminous red galaxy and QSO survey (2SLAQ: Croom et al. 2009) across the ∼16 deg^2 field. A statistical background subtraction was performed on the measured fluxes for each QSO to account for confusion in the maps (see Bonfield et al. 2011). Of the 372 QSOs, ∼20 per cent are consistent with having $L_{\rm FIR} \geq 10^{12}\,{\rm L}_{\odot}$, making them candidates for 'transition' QSOs (e.g. between an FIR-bright SMG and FIR-faint unobscured QSO phase). Restricting the redshift range to $z = 2$–3 (to roughly match the redshift peak of SMGs; Chapman et al. 2005) gives 29 QSOs. We then estimated SMBH masses for these QSOs from the extrapolated rest-frame 5100-Å luminosities (e.g. Wandel et al. 1999) to select those with SMBH masses of $M_{\rm BH} \lesssim 3 \times 10^8\,{\rm M}_{\odot}$, comparable to SMGs (Alexander et al. 2008). These selection criteria resulted in nine targets and from this list we selected six QSOs for a project to determine their gas masses and dynamics through the detection of ^{12}CO (3–2) emission with PdBI. We estimated systemic redshifts for these QSOs using the measured wavelengths from Gaussian fits to the Si IV 1397, C IV 1549 and C III] 1909 emission lines in their spectra (Fig. 1). We then adjust our estimates by the weighted mean velocity offsets of these lines from ^{12}CO (3–2), for the ^{12}CO-detected QSOs in Coppin et al. (2008); we find Si IV 1397 provides the best estimate of the systemic redshifts. We note that, as previously seen by Omont et al. (1996), roughly ∼80 per cent of these FIR-bright QSOs show very weak Lyα emission (Fig. 1). There may be a relation between FIR luminosity and weak Lyα, but its physical origin is still unknown.

This paper presents the PdBI observations of two QSOs from this sample: J0908−0034 (RA: $09^{\rm h}08^{\rm m}47\overset{\rm s}{.}18$; Dec.: $-00^\circ34'17\overset{''}{.}9$; J2000; $z_{\rm UV} = 2.5073$) and J0911+0027 (RA: $09^{\rm h}11^{\rm m}48\overset{\rm s}{.}38$; Dec.: $+00^\circ27'19\overset{''}{.}7$, J2000; $z_{\rm UV} = 2.3697$). Due to scheduling priorities, the remaining four targets in the sample have not yet been completed. In this paper, we therefore combine our observations with literature values for ^{12}CO (3–2)-detected FIR-bright QSOs, creating a sample from which we can study the population as a whole. As discussed earlier, the limitations of previous studies means the literature values do not easily relate to the typical SMG and, due to their large SMBH masses, are considered statistical outliers in the evolutionary scenario we propose. In Section 4, we discuss our observations and their agreement with a simple evolutionary model linking SMGs and QSOs.

2.2 PdBI observations

We used the six-element IRAM PdBI in compact (D) configuration to search for redshifted ^{12}CO (3–2) emission from the QSOs. We tuned the correlator WideX to the frequency of redshifted ^{12}CO (3–2) from the estimated redshifts derived from their UV emission lines (Fig. 1): 98.593 and 102.619 GHz for J0908−0034 and J0911+0027, respectively. The advantage of WIDEX is that its 3.6-GHz (dual polarization) spectral coverage, at a fixed channel spacing of 1.95 MHz, corresponds to a velocity range of ∼10 000 km s^{-1}, sufficient to identify the ^{12}CO (3–2) line even if the UV lines are significantly offset from the systemic redshift. We obtained a total on-source observing time of 6 h for each QSO between 2010 April 26 and 2010 May 4. The overall flux density scale was calibrated to 3C 273, with observations of J0906+015 for phase and amplitude calibration. Receiver bandpass calibration was performed on 0923+392. The data were calibrated in the GILDAS software package and a naturally weighted data cube produced for each QSO. In this configuration, the synthesized beam for natural weighting is 6.3×5.0 arcsec^2 at a position angle (PA) of 166° for J0908−0034 and 7.3×5.6 arcsec^2 at a PA of 19° for J0911+0027.

2.3 Far-infrared luminosities and SMBH masses

For our analysis, we derive more accurate estimates of the FIR luminosities and SMBH masses of our QSOs. To estimate FIR luminosities of the QSOs in our sample, we exploit the *Herschel* SPIRE 250-, 350- and 500-μm imaging. For each QSO, we deblend multiple sources in the vicinity, using the 250-μm map to identify nearby sources. For J0911+0027, there is a bright 250-μm source centred at the optical position of the QSO which is clearly isolated, but J0908−0034 has significant (40–60 per cent at 250–500 μm) contamination from a galaxy ∼30 arcsec away. We report the final deblended photometry for each source in Table 1. To derive the FIR luminosity for each QSO, we fit a modified blackbody spectra to the SPIRE photometry, adopting a dust emissivity $\beta = 1.6$ and fixing the temperature of the modified blackbody at $T_{\rm d} = 40$ K (the average dust temperature of $z \sim 2$–3 QSOs; Beelen et al. 2006), and calculate the FIR luminosity ($L_{\rm FIR}$) by integrating the best-fitting Spectral Energy Distribution (SED) between (rest-frame) 8 and 1000 μm. We note that if we instead allow the characteristic dust temperature to vary in the SED fit, we see at most a ∼45 per cent change in $L_{\rm FIR}$, consistent within our error estimates. The modified blackbody fits confirm that the $L_{\rm FIR}$ for both QSOs is $\sim(3\text{–}4 \pm 1) \times 10^{12}\,{\rm L}_{\odot}$ (Table 2). In comparison, the median $L_{\rm FIR}$ for the QSO sample of Coppin et al. (2008) is $L_{\rm FIR} = (7.5 \pm 1.5) \times 10^{12}\,{\rm L}_{\odot}$, and for SMGs

Table 1. Observed properties.

QSO	$\alpha_{\rm CO}$ (J2000)	$\delta_{\rm CO}$ (J2000)	$S_{250\,\mu{\rm m}}$ [a] (mJy)	$S_{350\,\mu{\rm m}}$ [a] (mJy)	$S_{500\,\mu{\rm m}}$ [a] (mJy)	$S_{3\,{\rm mm}}$ (mJy)
J0908−0034	09 08 47.18	−00 34 16.6	9.0 ± 6.6	26.2 ± 8.1	15.0 ± 9.0	<1.4
J0911+0027	09 11 48.30	+00 27 18.4	25.3 ± 5.8	14.7 ± 6.6	7.7 ± 7.8	<1.0

[a]J0908−0034 flux density values are after deblending sources. Fluxes extracted at the optical position of the QSO, before deblending, are 15.6 ± 6.4, 39.5 ± 7.1 and 41.0 ± 8.5 mJy.

Table 2. Physical properties.

Source	$z_{\rm CO}$	$S_{\rm CO}\Delta v$ (Jy km s^{-1})	FWHM$_{\rm CO}$ (km s^{-1})	$L'_{\rm CO\,(3-2)}$ (10^{10} K km s^{-1} pc^2)	$L_{\rm FIR}$ (10^{12} L$_\odot$)	$M_{\rm gas}$ (10^{10} M$_\odot$)	$M_{\rm BH}$ (10^8 M$_\odot$)
J0908−0034	2.5008 ± 0.0002	0.23 ± 0.04	125 ± 25	0.77 ± 0.15	3.1 ± 0.8	0.77 ± 0.15	$1.6^{+0.3}_{-0.2}$
J0911+0027	2.3723 ± 0.0005	0.62 ± 0.10	530 ± 100	1.9 ± 0.3	3.5 ± 0.8	1.9 ± 0.3	$2.5^{+1.4}_{-0.9}$

in Bothwell et al. (2012) it is $L_{\rm FIR} = (4.8 \pm 0.6) \times 10^{12}\,{\rm L}_\odot$. The implied star formation rates[3] (SFRs) are 500–700 M$_\odot$ yr^{-1}.

Similarly, we calculated SMBH masses for both QSOs from the full width at half-maximum (FWHM) of their C IV 1549 emission lines and their rest-frame 1350-Å continuum luminosities (L_{1350}), following equation (7) from Vestergaard & Peterson (2006). This relation is calibrated to the results of reverberation mapping; however, the geometry of the broad-line region (producing the emission lines) is poorly constrained and we caution it may bias virial mass estimates to low values (Jarvis & McLure 2006; Fine, Jarvis & Mauch 2011). Nevertheless, we derive the FWHM from a Gaussian fit to the C IV emission line in the 2SLAQ spectra (Fig. 1), measuring 4500 ± 340 and 5900^{+1600}_{-1300} km s^{-1} for J0908−0034 and J0911+0027, respectively, and determine L_{1350} from the g-band SDSS magnitudes of $g = 21.41 \pm 0.05$ for J0908−0034 and $g = 21.64 \pm 0.05$ for J0911+0027. As we do not see strong evidence of reddening in the 2SLAQ spectrum of either QSO, we do not consider the effects of dust extinction on our estimates of L_{1350} (Fig. 1). From these, we estimate SMBH masses of $\sim 2 \times 10^8$ M$_\odot$ for both QSOs[4] (Table 2). We caution that estimates from the C IV emission line can overpredict the SMBH mass by a factor of 2–5, when compared to estimates from Hα (Ho et al. 2012). In the absence of a more robust mass estimator, we simply acknowledge that the SMBH masses of our sources may be overestimated.

3 ANALYSIS AND RESULTS

We detect ^{12}CO emission near the optical position of each QSO (within $\lesssim$1–2 arcsec) and at frequencies close to those expected for redshifted ^{12}CO (3–2). For each QSO, we fit a combination of a Gaussian and a uniform continuum to the spectrum corresponding to the peak signal-to-noise ratio (S/N) pixel in each map and report the resulting redshift, linewidth and line flux in Table 2, as well as overplotting the fit on Fig. 2. We detect no significant continuum emission at 3 mm in either QSO (3σ limits given in Table 1), which is consistent with no contribution from synchrotron emission to the FIR luminosities of these systems. The quoted errors were obtained from a bootstrap error analysis on the model fit to the data. The resulting values of χ^2 indicate good fits to both emission lines: $\chi^2_{\rm r} = 1.0$ for J0908−0034 and $\chi^2_{\rm r} = 1.1$ for J0911+0027. Previous results have found that ∼25 per cent of SMGs display a double-peaked emission line, with a velocity difference between peaks $\gtrsim$500 km s^{-1} (Greve et al. 2005; Tacconi et al. 2006; Engel et al. 2010; Bothwell et al. 2012), indicating either a merger or disc-like kinematics. To test for this, we attempt to fit a double Gaussian model to the spectra in Fig. 2. We find it produces a negligible improvement in χ^2, and conclude that single Gaussian fits are sufficient to describe the line profiles of both QSOs.

We collapse the spectral cube over the frequency range corresponding to ± FWHM of the emission line to create the maps of the ^{12}CO (3–2) emission shown in Fig. 2. These maps are continuum subtracted, although as we noted above no significant continuum is detected in either source. We now discuss the ^{12}CO (3–2) emission-line properties of each QSO in more detail.

J0908−0034. The integrated ^{12}CO (3–2) emission is detected at an S/N of 5.5σ. The ^{12}CO emission line is relatively narrow and so we bin to a frequency resolution of 10 MHz (∼30 km s^{-1}), as shown in Fig. 2. We find the ^{12}CO (3–2) emission line to be well fitted by a single Gaussian with FWHM $= 125 \pm 25$ km s^{-1} and a velocity-integrated flux of $S_{\rm CO}\Delta v = 0.23 \pm 0.05$ Jy km s^{-1} (see Table 2). From the peak of the Gaussian distribution, we determine a ^{12}CO redshift of $z = 2.5008 \pm 0.0002$. We compared $z_{\rm CO}$ with the wavelength of emission lines in the 2SLAQ spectrum of this QSO (Fig. 1). We found the UV lines to be blueshifted by $\Delta v \sim$ 100–500 km s^{-1}, relative to $z_{\rm CO}$, with Lyα and N V emission lines having the largest offset. Systematic offsets of UV emission lines are not unusual, and are usually attributed to resonant scattering of the emission line, due to material in the line of sight to the AGN (Steidel et al. 2010). At the spatial resolution of our D-configuration PdBI observations, we do not find any evidence for spatially resolved ^{12}CO (3–2) emission, and channel maps show no sign of a velocity gradient across the source.

J0911+0027. The integrated ^{12}CO emission is detected at a significance of 7.2σ. The ^{12}CO (3–2) spectrum is binned to a frequency resolution of 20 MHz (∼60 km s^{-1}), as shown in Fig. 2. We find the ^{12}CO (3–2) emission line to be well fitted by a single Gaussian distribution with FWHM $= 530 \pm 100$ km s^{-1} and a velocity-integrated flux of $S_{\rm CO}\Delta v = 0.62 \pm 0.10$ Jy km s^{-1} (see Table 2). We determine a ^{12}CO redshift of $z = 2.3723 \pm 0.0005$ from the line fit. The rest-frame UV emission lines in the 2SLAQ spectrum of this QSO are blueshifted by $\Delta v \sim$ 500–1500 km s^{-1}, relative to $z_{\rm CO}$ (Fig. 1). As

[3] SFR (M$_\odot$ yr^{-1}) $= 1.7 \times 10^{-10}\,L_{\rm FIR}$ (L$_\odot$) (Kennicutt 1998), following a Salpeter initial mass function over a mass range 0.1–100 M$_\odot$.

[4] We estimate errors by bootstrap resampling the 2SLAQ spectrum, with replacement, and refitting a Gaussian model.

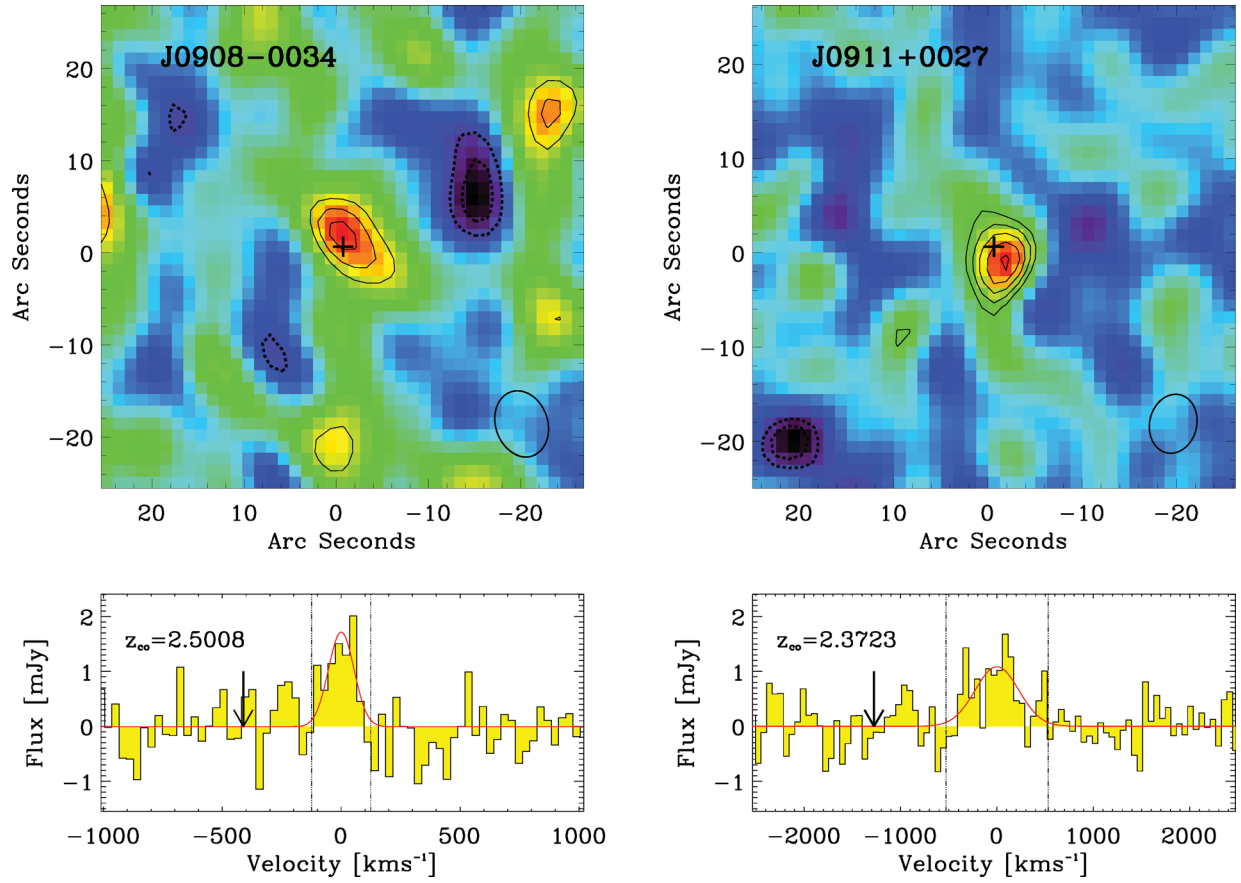

Figure 2. Upper: the velocity-integrated ^{12}CO (3–2) emission for the two QSOs (summed over the regions marked in the spectra below). The contours represent signal-to-noise ratio, and are spaced at $\pm3\sigma$, 4σ, 5σ, ... (dashed contours are negative). Significant ^{12}CO (3–2) emission is detected from both QSOs and is well centred on the optical positions of the QSOs, indicated by a cross (offset by 1–2 arcsec, which is within the primary beam). Analysis of the channel maps shows both sources are unresolved with no evidence of velocity gradients, although the modest spatial resolution of our maps means that this is not a strong constraint. Lower: spectra showing the redshifted ^{12}CO (3–2) emission lines from both QSOs. The spectra were binned to a resolution of 10 and 20 MHz, respectively, and we overlay the best-fitting Gaussian plus continuum model (the continuum emission in both QSOs is negligible). The redshift derived from ^{12}CO (3–2) and the line flux and linewidths derived from the Gaussian fits are reported in Table 2. We note that the FWHM of the J0908−0034 emission line is relatively narrow, at 125 ± 25 km s^{-1}, compared to 530 ± 100 km s^{-1} for J0911+0027. In each spectrum, the predicted position of the ^{12}CO (3–2) emission line, from the 2SLAQ UV spectrum, is indicated by an arrow. The two triple dot–dashed lines correspond to ±FWHM, and show the region which was summed to produce the maps above.

with J0908−0034, Lyα and N v emission lines display the largest offsets, but strong absorption in Lyα and N v may affect the accuracy of the Gaussian fit to the emission lines. At the low spatial resolution of our D-configuration observations, there is no evidence for spatially resolved ^{12}CO (3–2) emission, and again the channel maps do not show any indication of velocity gradients across the line.

We now compare our observations of these two FIR-luminous, but otherwise fairly typical, QSOs with the more luminous (and more massive) FIR-bright QSOs previously studied, as well as with the SMG population. In particular, we investigate what the observed properties of our QSOs can tell us about their relationship to SMGs.

3.1 Gas mass

The ^{12}CO (3–2) line emission from each QSO provides information about the molecular gas mass of the system (Solomon et al. 1997). We determine the ^{12}CO (3–2) line luminosity, $L'_{\rm CO\,(3-2)}$, following equation (3) from Solomon & Vanden Bout (2005), deriving $L'_{\rm CO\,(3-2)} = (0.77 \pm 0.15) \times 10^{10}$ and $(1.9 \pm 0.3) \times 10^{10}$ K km s^{-1} pc^2 for J0908−0034 and J0911+0027, respectively (Table 2).

To estimate the total masses of the gas reservoirs in these QSOs, we use the ^{12}CO (3–2) luminosity to determine the expected ^{12}CO (1–0) luminosity and from that derive the total gas mass. For the first step, we must adopt a line brightness ratio, $r_{31} = L'_{\rm CO\,(3-2)}/L'_{\rm CO\,(1-0)}$, to convert the ^{12}CO (3–2) line luminosity to a ^{12}CO (1–0) luminosity. Bothwell et al. (2012) determine that for SMGs $r_{31} = 0.52 \pm 0.09$, which reflects the presence of an extended reservoir of cold gas. However, recent results indicate that such an extended reservoir is not present in QSOs, and as such we follow the results of Riechers et al. (2011) and adopt a value of $r_{31} = 1.0$ (i.e. thermalized gas) in the conversion for both our QSOs and the QSO sample of Coppin et al. (2008). We caution that this assumption has not been tested for our sample of QSOs, and in fact in AGN-dominated systems superthermal ratios, i.e. $r > 1$, are not uncommon (e.g. Papadopoulos et al. 2008; Ivison et al. 2012). We then adopt a CO-to-H_2 conversion factor of $\alpha = 1\,{\rm M}_\odot\,({\rm K\,km\,s^{-1}\,pc^2})^{-1}$ following Solomon & Vanden Bout (2005) to convert $L'_{\rm CO}$ (1–0) to a gas mass. Note that α is denoted as a conversion to H_2, but the resulting H_2 mass is defined as the total H_2+He gas mass. For ease of comparison, we adopt the same value for α used in the SMG survey of Bothwell et al. (2012), and for consistency we scale the gas

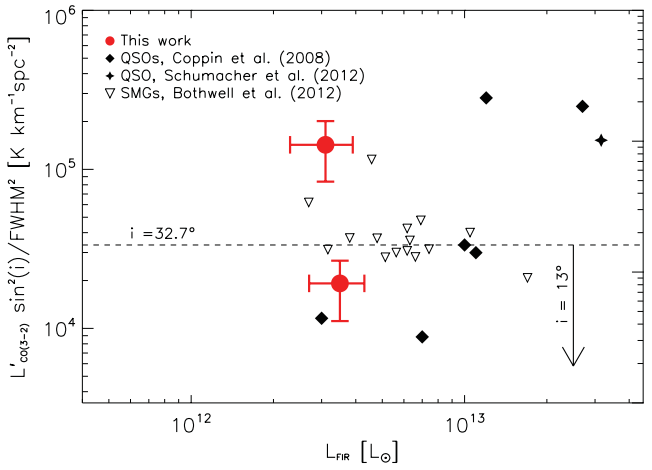

Figure 3. The variation in $L'_{\rm CO(3-2)}\sin^2 i/{\rm FWHM}^2$, a proxy for molecular gas-mass fraction, as a function of FIR luminosity, for high-redshift QSOs and SMGs. We adopt a mean inclination for both populations, of 32.°7, appropriate for randomly orientated discs. For each sample, we determine the median, but given the similarity of the results, we show only the QSO value (dashed line). Our proxy for gas-mass fraction assumes that the gas reservoirs in QSOs and SMGs have the same geometry, physical radius and mean inclination on the sky. We do not expect SMGs to suffer an inclination bias, but this may not be true for the optically identified QSOs we study here, as the identification is based on their broad-line properties. We indicate with an arrow the effect of adopting a mean inclination of 13° for the QSO population, which may be more realistic (see Section 3.2). One of our targets, J0908−0034, has an unusually narrow emission line, indicating the galaxy is observed close to face-on. By adopting an average inclination, we may be deriving a low dynamical mass, and hence a high gas fraction, for this source. Our proxy also assumes that the populations have the same line brightness ratio (see Section 3.1). A value of $r_{31} = 0.52$ is more appropriate for SMGs, and would further increase the separation between the implied gas-mass fractions of SMGs and QSOs, with the latter having lower gas fractions and hence appearing more evolved.

masses quoted in Coppin et al. (2008) to this value. In this manner, we derive gas masses of $M_{\rm gas} = (0.77 \pm 0.15) \times 10^{10}$ and $(1.9 \pm 0.3) \times 10^{10}\,{\rm M}_\odot$ for J0908−0034 and J0911+0027, respectively.

The gas masses of our FIR-luminous QSOs are lower than the median gas mass of the typically more FIR-luminous QSOs detected by Coppin et al. (2008), $M_{\rm gas} = (4.3 \pm 1.0) \times 10^{10}\,{\rm M}_\odot$, and they are also lower than the median gas mass of SMGs from Bothwell et al. (2012), $M_{\rm gas} = (5.3 \pm 1.0) \times 10^{10}\,{\rm M}_\odot$. We note that there is significant scatter around these averages. As we will discuss in Section 4, the lower gas masses we derive for our FIR-luminous QSOs are consistent with them having recently evolved from a previous SMG phase.

3.2 Gas fraction

One rough measure of the evolutionary state of a system is the fractional contribution of molecular gas to its total mass. Hence, in the absence of significant replenishment of gas from external sources, we would expect the gas-mass fraction in SMGs to decline as they evolve, and thus in the evolutionary model we are testing, our QSOs ought to have lower gas-mass fractions than SMGs.

In Fig. 3, we use a combination of observables which trace gas mass, $L'_{\rm CO(3-2)}$, and dynamical mass, ${\rm FWHM}^2/\sin^2 i$, as a proxy for gas-mass fraction, $L'_{\rm CO(3-2)}\sin^2 i/{\rm FWHM}^2$. In choosing this proxy, we make two implicit assumptions: (i) that the conversion of $L'_{\rm CO(3-2)}$ to $M_{\rm gas}$ is the same for SMGs and QSOs, i.e. the populations have the same value of r_{31} and α, and (ii) the physical extent, and orientation, of the reservoir is similar in both populations. Fig. 3 shows that the FIR-bright QSOs have similar values of $L'_{\rm CO(3-2)}\sin^2 i/{\rm FWHM}^2$ on average to SMGs. To determine if this means that they have similar gas-mass fractions (potentially indicating they are not more evolved), we need to consider the two simplifying assumptions above.

It is believed that SMGs do not suffer from an inclination selection bias as their submm emission is optically thin and so, if we are modelling their gas distributions as disc-like systems (Swinbank et al. 2011), we can adopt a mean inclination of 32.°7, appropriate for randomly orientated discs (Bothwell et al. 2012). Recent studies comparing ^{12}CO linewidths of QSOs and SMGs found no distinction between the populations, indicting that they have the same average inclination (Coppin et al. 2008). As such, in our analysis we adopt the same average inclination for QSOs and SMGs. However, optically identified QSOs such as those studied here may have preferentially biased orientations, as to have identified them as QSOs we must be able to observe their broad-line regions. If we adopt a mean inclination of 13°, which has been previously suggested (Carilli & Wang 2006), then the QSO sample has an ∼85 per cent lower gas-mass fraction, on average, than the SMGs. While the difference is significant at only 2.0σ, it is in the sense expected if QSOs are more evolved systems. We note that one of our targets, J0908−0034, has an unusually narrow linewidth for a high-redshift galaxy, indicating we may be observing the system close to face-on. By assuming an average inclination of 32.°7, we may be deriving a low dynamical mass and hence significantly overestimating the gas fraction for this source.

Our proxy for gas-mass fraction also assumes that the conversion from $L'_{\rm CO(3-2)}$ to gas mass is the same for both the QSO and SMG populations, which is a conservative assumption. If instead we were to include the differences in line brightness temperature ratio (r_{31}), expected for the two populations ($r_{31} = 1.0$ for QSOs and $r_{31} = 0.52$ for SMGs), then the gas-mass fraction is roughly doubled in SMGs, and as a result the offset between the populations in Fig. 3 becomes larger and the statistical significance of the difference increases to 3.6σ (including a bias in the QSO inclination). We conclude that although the estimated gas-mass fractions of FIR-bright QSOs appear similar to typical SMGs, after adopting reasonable assumptions for the excitations and orientations of the two populations there is evidence of a difference in their gas fractions.

3.3 Gas consumption time-scales

A second important measure of the evolutionary state of SMGs and QSOs comes from their gas consumption time-scales: $M_{\rm gas}/{\rm SFR}$ (or the inverse of this: the star formation efficiency). In our evolutionary scenario, the gas reservoir in SMGs is depleted by star formation as they transform from dusty systems to unobscured QSOs. Our 'transition' FIR-bright QSOs are expected to represent a unique evolutionary phase, with prodigious star formation but lower gas masses, and thus shorter gas consumption time-scales.

The ratio of the observables, ^{12}CO (3–2) line luminosity, $L'_{\rm CO(3-2)}$, and FIR luminosity, $L_{\rm FIR}$, can be used as a proxy for the gas consumption time-scale of a galaxy. This ratio has the advantage that we do not make any assumptions in the conversion of ^{12}CO (3–2) measurement to ^{12}CO (1–0). We have therefore gathered samples of SMGs and FIR-bright QSOs which have been detected in ^{12}CO (3–2), allowing a direct comparison of observable quantities. We use literature values for the ^{12}CO (3–2) luminosities of QSOs

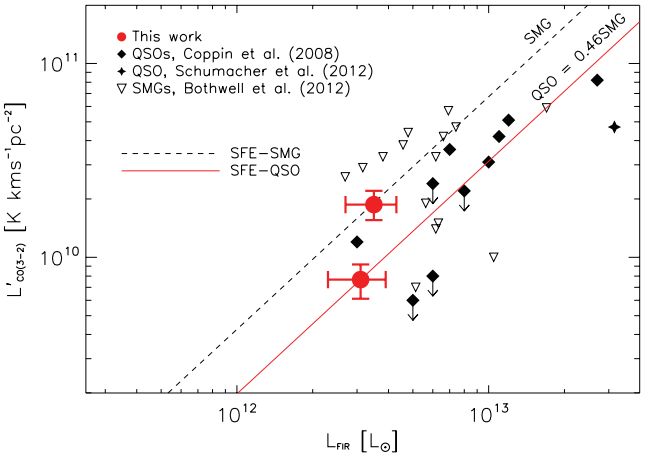

Figure 4. ^{12}CO (3–2) line luminosity ($L'_{\rm CO\,(3-2)}$) versus FIR luminosity ($L_{\rm FIR}$) for FIR-bright QSOs and ^{12}CO (3–2)-detected SMGs. We plot the best-fitting line to the SMG population and we fix the gradient of the fit to the QSOs to that measured for the SMGs, $dL'_{\rm CO\,(3-2)}/dL_{\rm FIR} = 1.2 \pm 0.3$ (Bothwell et al. 2012). We treat upper limits in our QSO sample as detections, and as such the fit is a conservative upper estimate. At a fixed $L_{\rm FIR}$, the QSOs have $L'_{\rm CO\,(3-2)}$ which is a factor of $\sim$50 ± 30 per cent lower than the SMGs. A two-sided KS test indicates a 99.3 per cent probability that the $L'_{\rm CO(3-2)}/L_{\rm FIR}$ ratio for SMGs and QSOs are drawn from a different parent distribution. If we take into account the difference in the line brightness temperature ratios, r_{31}, for the two populations, then this probability increases to 99.95 per cent. The differences in the populations are in the sense that the FIR-bright QSOs appear to have shorter gas consumption time-scales, consistent with representing a subsequent evolutionary phase.

(Beelen et al. 2004; Coppin et al. 2008; Schumacher et al. 2012) and ^{12}CO (3–2)-detected SMGs (Bothwell et al. 2012). We plot our QSOs along with these comparison samples in Fig. 4, and overlay the best-fitting line to each sample. To test for an offset between the populations, we fix the gradient of each line at 1.2 ± 0.3, which is the best-fitting value to ^{12}CO (3–2) SMGs (Bothwell et al. 2012). We also caution that when fitting a line to the sample, upper limits are treated as detections. If any of these non-detections have significantly lower values of $L'_{\rm CO(3-2)}$, then the offset to the SMG population, seen in Fig. 4, will increase. We see that our observations follow a similar trend to the literature QSO values. Combining our results with the QSO sample, we find $\sim$50 ± 30 per cent[5] lower ratios of $L'_{\rm CO(3-2)}/L_{\rm FIR}$ than SMGs, potentially indicating shorter gas consumption time-scales. To test if the SMGs and QSOs are also drawn from the same parent distribution, we perform a two-sided Kolmogorov–Smirnov (KS) test on the ratio $L'_{\rm CO(3-2)}/L_{\rm FIR}$. The KS test returns a value of 0.7 per cent, indicating a small probability that the populations are drawn from the same parent distribution; however, we stress that this interpretation implicitly assumes the same value for r_{31} in the two populations.

^{12}CO (3–2) emission traces warm and/or dense environments; hence, to convert $L'_{\rm CO(3-2)}$ to a total gas mass we must make assumptions about the temperature distribution within the gas. In QSOs, it is thought that the gas is close to thermal equilibrium, meaning that the ^{12}CO (3–2) transition traces the majority of the gas in the system (Riechers et al. 2011). Bothwell et al. (2012) show that the ^{12}CO($J, J-1$), $J \geq 2$, emission lines in SMGs are subthermally excited (see also Harris et al. 2010), which is interpreted as an indication for the presence of multiple temperature components: a warm component associated with the star-forming regions and a cooler component associated with extended, quiescent, gas (see also Danielson et al. 2011). If we use the proposed r_{31} value for QSOs, $r_{31} = 1.0$, and for SMGs, $r_{31} = 0.52$, the fixed offset between the two populations will increase, as the SMG gas masses roughly double relative to the QSOs. A two-sided KS test, including these values, returns a 0.05 per cent probability that the SMG and QSO gas-mass time-scales are drawn from the same parent distribution. Thus, it appears that the FIR-bright QSOs not only lack the extended, cool reservoir of gas seen in SMGs (e.g. Ivison et al. 2010, 2011), but also have less warm/dense gas than SMGs, suggesting that they are more evolved.

The lower ratio of $L'_{\rm CO(3-2)}/L_{\rm FIR}$ for our sample compared to SMGs is in disagreement with the results of Coppin et al. (2008), who do not find evidence for a fixed offset between their sample of extremely FIR-bright QSOs and the SMG sample of Greve et al. (2005). However, the reason for this discrepancy is likely due to the choice of SMG comparison samples used in the two analyses. For example, Coppin et al. (2008) compared their results to the Greve et al. (2005) sample which contains 18 SMGs, of which only four are unlensed ^{12}CO (3–2)-detected sources [as such, in their analysis, Coppin et al. (2008) create an SMG sample which contains 17 sources, observed in mix of CO transitions, and converted to a single CO transition by assuming the gas is thermalized]. In contrast, we make use of the recent SMG survey of Bothwell et al. (2012), which contains 15 unlensed ^{12}CO (3–2)-detected SMGs. Since we are now in a position to compare our QSOs to only ^{12}CO (3–2)-detected, unlensed, SMGs, this removes some of the uncertainty associated with combining samples observed in different transitions and leads to a different conclusion.

4 DISCUSSION

In order to study the link between QSOs and SMGs, we have selected two FIR-detected QSOs at $z \sim 2.5$ (the epoch of peak activity in SMG and QSO populations) whose SMBH masses ($\sim 2 \times 10^8$ M$_\odot$) are comparable to the average SMBH mass for the SMG population (Alexander et al. 2008). In contrast, the majority of previously ^{12}CO-detected (unlensed) FIR-bright QSOs have $M_{\rm BH} \sim 10^9$–10^{10} M$_\odot$ (Coppin et al. 2008), so much larger than the average SMG $M_{\rm BH}$ that they cannot have recently evolved from a typical SMG (as pointed out by Coppin et al. 2008). It is precisely this mismatch in SMBH masses which our study addresses. Given their FIR luminosities and SMBH masses, our new sample is a more accurate representation of the typical FIR-bright QSO population and hence can be used to test an evolutionary link between SMGs and QSOs, through their gas and dynamical masses, as traced by their ^{12}CO (3–2) emission.

We show in Fig. 5 the distribution of estimated gas and SMBH masses for our two QSOs, as well as the average ^{12}CO (3–2)-detected SMG from Bothwell et al. (2012) and the QSO sample from Coppin et al. (2008). We again note that gas masses are calculated by adopting $r_{31} = 1.0$ for QSOs and $r_{31} = 0.52$ for SMGs, which are the appropriate values for each population. To investigate how galaxies might evolve with time, we follow Coppin et al. (2008) and overlay a simple evolutionary model based on gas consumption and SMBH growth time-scales. We take the average SFR of SMGs from Bothwell et al. (2012) as 500 M$_\odot$ yr^{-1} and use this to calculate the reduction in their gas mass with time. In this simple model, we assume a constant SFR and do not include mass loss due to winds. By selection our QSOs have SMBH masses similar to the average SMGs, but to estimate the growth of the central SMBH

[5] Error estimated by bootstrap resampling.

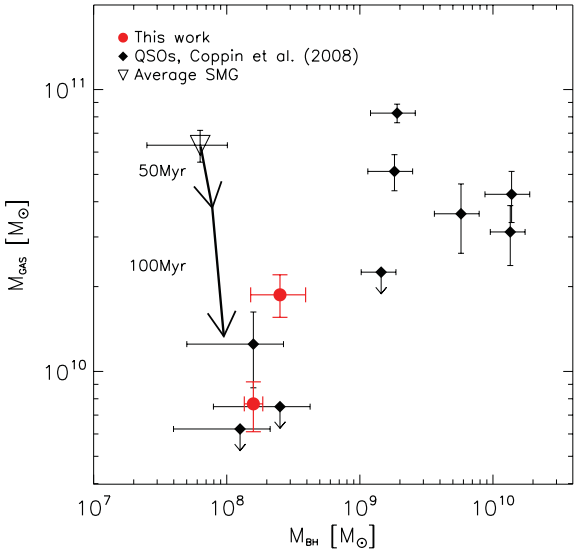

Figure 5. A comparison of gas and SMBH masses for FIR-bright QSOs and SMGs which have been observed in ^{12}CO (3–2). The QSO points are taken from Coppin et al. (2008, including literature values from Beelen et al. 2004), the average SMG gas mass from Bothwell et al. (2012) and SMBH mass from Alexander et al. (2008). The gas masses are derived from the ^{12}CO (3–2) line luminosity, using the appropriate r_{31} for each population (see Section 3.1). We show the predicted evolution of the gas mass and SMBH mass in a model SMG in which star formation and SMBH growth occur in tandem for a period of 50 or 100 Myr. For the star formation, we assume a constant rate of 500 $M_\odot$ yr^{-1} (Bothwell et al. 2012). The growth of the SMBH is calculated following equation (10) from Alexander & Hickox (2012), and we assume it is accreting with an Eddington ratio of $\eta = 0.2$ (Alexander et al. 2008). We conclude that the properties of the FIR-bright QSOs in our sample, and the QSOs with $M_{\rm BH} < 10^9\,M_\odot$ from Coppin et al. (2008), are consistent with their recent evolution from an earlier SMG-like phase. The FIR-bright QSOs with $M_{\rm BH} > 10^9\,M_\odot$ are attributed as statistical outliers in this evolutionary scenario, as their SMBH masses are amongst the largest seen in the local Universe.

on the gas consumption time-scale we follow equation (10) from Alexander & Hickox (2012). In line with the measured properties of SMGs, we limit the growth to an Eddington ratio, $\eta = 0.2$,[6] and an efficiency of 0.1 (Alexander et al. 2008); this then predicts the estimated growth in the SMBH mass in parallel to the depletion of the gas reservoir.

In Fig. 5, we plot tracks showing the evolution in the expected gas and SMBH masses for the descendents of SMGs after 50 and 100 Myr. As can be seen, after 100 Myr the SMGs in this model are expected to have almost completely depleted their gas reservoirs and will have gas masses comparable to those we detect in the FIR-luminous QSOs. At the same time, their SMBHs will have grown by ∼50 per cent, resulting in masses similar to those seen in our target QSOs. As can be seen from Fig. 5, the rate of growth of the SMBH and the depletion of the gas reservoir can link the properties of a typical SMG to those seen in our FIR-bright QSOs around ∼100 Myr later.

Are all SMGs likely to go through a QSO phase? If these three $z \sim 2$–3 populations (i.e. $S_{850\,\mu\rm m} \gtrsim 5$ mJy SMGs and QSOs with SMBH with masses $\gtrsim 10^8\,M_\odot$, which are both FIR bright and faint) are uniquely related through a simple evolutionary cycle, then the product of their respective space densities and lifetimes should be similar. On average, we expect the SMG lifetimes to be comparable to their gas depletion time-scales (Fig. 5) or $\sim 10^8$ yr (Swinbank et al. 2006; Hickox et al. 2012) and their volume density at $z \sim 2$–3 is $\sim 10^{-5}$ Mpc^{-3} (e.g. Wardlow et al. 2011). In comparison, the QSO volume density at $z \sim 2$–3 (with SMBH masses above $\sim 10^8\,M_\odot$) is $\sim 10^{-6}$ Mpc^{-3} (Croom et al. 2009) and estimates of their lifetimes are $\gtrsim$10 Myr (Martini & Weinberg 2001; Hosokawa 2002). As noted by a number of previous authors, the space densities and duty cycles of these populations are thus consistent with all SMGs subsequently transforming into a QSO.

If they transform through an FIR-bright QSO phase, how long can this be? From Chapman et al. (2005) and Wardlow et al. (2011), we estimate that FIR-bright QSOs have a volume density at $z \sim 2$–3 of $\sim 10^{-7}$ Mpc^{-3}. By comparison to the SMG and QSO lifetimes, this implies a duration for this transition phase of just ∼1 Myr. Estimates of lifetimes and space densities for each population are uncertain at $\gg 2\times$, and so a qualitative agreement is reasonable. If the QSO influences its host through winds and outflows with characteristic velocities of ∼1000 km s^{-1} (e.g. Harrison et al. 2012), then the estimated duration of the FIR-bright phase would allow these winds to reach kpc scales, comparable to the likely extent of the gas reservoirs and star formation activity within these systems (e.g. Tacconi et al. 2008; Ivison et al. 2011). This may help explain the short duration of the 'transition' phase, although it may be exhaustion of the gas reservoir by star formation which is allowing these winds to propagate freely.

5 CONCLUSIONS

The main conclusions from our study are the following.

(i) We have used IRAM PdBI to search for redshifted ^{12}CO (3–2) emission from two FIR-bright QSOs at $z \sim 2.5$ selected from the H-ATLAS survey. These QSOs were selected to have SMBH masses of $M_{\rm BH} \leq 3 \times 10^8\,M_\odot$, which are more comparable to typical SMGs than those in samples of high-redshift FIR-luminous QSOs previously detected in ^{12}CO. Our observations detect ^{12}CO (3–2) emission from both QSOs and we derive line luminosities of $L'_{\rm CO(3-2)} = (0.77 \pm 0.15) \times 10^{10}$ and $(1.9 \pm 0.3) \times 10^{10}$ K km s^{-1} pc^2 for J0908−0034 and J0911+0027, respectively (Table 2).

(ii) Comparing our FIR-bright QSOs (and similar systems from the literature) with SMGs, we find that the QSOs have similar values of $L'_{\rm CO(3-2)} \sin^2 i/{\rm FWHM}^2$, our proxy for gas-mass fraction, to SMGs. However, this is subject to a number of assumptions. If we consider that QSOs have a biased inclination angle of 13°, as has been suggested (Carilli & Wang 2006), then the QSOs have an ∼85 per cent lower gas-mass fraction, at a significance of 2.0σ. In the absence of gas replenishment, this is consistent with QSOs being more evolved systems. Furthermore, adopting the appropriate line brightness ratios for each population roughly doubles the gas mass in SMGs, increasing this difference further, to a significance of 3.6σ. Therefore, with plausible assumptions there appears to be evidence for evolution in the gas fraction, but we require spatially resolved ^{12}CO (1–0) observations to test this conclusively.

(iii) By comparing the gas consumption time-scales, estimated from $L'_{\rm CO(3-2)}/L_{\rm FIR}$, for FIR-bright QSOs with SMGs, we find that the QSOs have $\sim 50 \pm 30$ per cent lower consumption time-scales. A two-sided KS test returns a 0.7 per cent probability that the populations are drawn from the same parent distribution, and adopting appropriate line brightness ratios, of $r_{31} = 1$ for QSO and

[6] $\eta = 0.2$ indicates fast black hole growth. Within uncertainties it is feasible the growth is Eddington limited, $\eta = 1$.

$r_{31} = 0.52$ for SMGs, decreases this to 0.05 per cent. We conclude that FIR-bright QSOs appear to have a lower mass of warm/dense gas [probed directly through ^{12}CO (3–2)]. Combined with previous results (Riechers et al. 2011), showing that QSOs also lack an extended, cool reservoir of gas seen in SMGs, we interpret this as evidence that the FIR-bright QSOs are at a different evolutionary stage than typical SMGs. In our evolutionary scenario, this is consistent with FIR-bright QSOs being in 'transition' from an SMG to a QSO.

(iv) We show that the gas and the SMBH masses in QSOs and SMGs are consistent with a model where SMGs transform into QSOs on a time-scale of $\sim$100 Myr. Furthermore, the relative volume densities and expected durations of the SMG and QSO phases are consistent with all SMGs passing through a subsequent QSO phase, and we estimate that the likely duration of the FIR-bright QSO phase is just $\sim$1 Myr. We note that if necessary this duration is still sufficient to allow the QSO to influence the star formation and gas reservoirs across the full extent of the host galaxy through 1000 km s^{-1} winds and outflows. To rigorously test this connection, we require ^{12}CO (1–0) observations, which would allow us to determine the gas reservoir masses of our QSOs, without making assumptions about the line brightness ratio, r_{31}.

The scale of this study is too small to single handedly prove or disprove an evolutionary link between SMGs and QSOs. However, the data we have obtained provide further evidence supporting the idea originally proposed by Sanders et al. (1988) that these populations are linked by an evolutionary sequence. We have compared ^{12}CO (3–2)-detected QSOs and SMGs through a number of observable quantities, and find that the time-scales for gas depletion, and SMBH growth, needed to link SMGs to these sources are consistent.

ACKNOWLEDGMENTS

This work is based on observations carried out with the IRAM PdBI. IRAM is supported by INSU/CNRS (France), MPG (Germany) and IGN (Spain). We thank Chiara Feruglio, Stephen Fine and Tom Shanks for help. JMS acknowledges the support of an STFC studentship. IRS, AMS and DMA acknowledge financial support from the STFC. IS acknowledges the support from a Leverhulme Fellowship. KEKC acknowledges support from the endowment of the Lorne Trottier Chair in Astrophysics and Cosmology at McGill, the Natural Science and Engineering Research Council of Canada (NSERC) and a L'Oréal Canada for Women in Science Research Excellence Fellowship, with the support of the Canadian Commission for UNESCO. The H-ATLAS is a project with *Herschel*, which is an ESA space observatory with science instruments provided by European-led Principal Investigator consortia and with important participation from NASA. The H-ATLAS website is http://www.h-atlas.org/.

REFERENCES

Alexander D. M., Hickox R. C., 2012, New Astron. Rev., 56, 93
Alexander D. M. et al., 2008, AJ, 135, 1968
Beelen A. et al., 2004, A&A, 423, 441
Beelen A., Cox P., Benford D. J., Dowell C. D., Kovács A., Bertoldi F., Omont A., Carilli C. L., 2006, ApJ, 642, 694
Birnboim Y., Dekel A., 2003, MNRAS, 345, 349
Blain A. W., Smail I., Ivison R. J., Kneib J.-P., Frayer D. T., 2002, Phys. Rep., 369, 111
Bonfield D. G. et al., 2011, MNRAS, 416, 13
Bothwell M. S. et al., 2012, MNRAS, submitted (arXiv:1205.1511)
Brown M. J. I. et al., 2008, ApJ, 682, 937
Carilli C. L., Wang R., 2006, AJ, 131, 2763
Chapman S. C., Blain A. W., Smail I., Ivison R. J., 2005, ApJ, 622, 772
Coil A. L. et al., 2008, ApJ, 672, 153
Coppin K. E. K. et al., 2008, MNRAS, 389, 45
Croom S. M. et al., 2002, MNRAS, 337, 275
Croom S. M. et al., 2009, MNRAS, 392, 19
Danielson A. L. R. et al., 2011, MNRAS, 410, 1687
Dekel A. et al., 2009, Nat, 457, 451
Di Matteo T., Springel V., Hernquist L., 2005, Nat, 433, 604
Eales S. et al., 2010, PASP, 122, 499
Engel H. et al., 2010, ApJ, 724, 233
Ferrarese L., Merritt D., 2000, ApJ, 539, L9
Fine S., Jarvis M. J., Mauch T., 2011, MNRAS, 412, 213
Frayer D. T., Ivison R. J., Scoville N. Z., Yun M., Evans A. S., Smail I., Blain A. W., Kneib J.-P., 1998, ApJ, 506, L7
Gebhardt K. et al., 2000, ApJ, 539, L13
Granato G. L., Silva L., Monaco P., Panuzzo P., Salucci P., De Zotti G., Danese L., 2001, MNRAS, 324, 757
Greve T. R. et al., 2005, MNRAS, 359, 1165
Griffin M. J. et al., 2010, A&A, 518, L3
Harris A. I., Baker A. J., Zonak S. G., Sharon C. E., Genzel R., Rauch K., Watts G., Creager R., 2010, ApJ, 723, 1139
Harrison C. M. et al., 2012, MNRAS, 426, 1073
Hartley W. G. et al., 2010, MNRAS, 407, 1212
Hickox R. C. et al., 2012, MNRAS, 421, 284
Ho L. C., Goldoni P., Dong X.-B., Greene J. E., Ponti G., 2012, ApJ, 754, 11
Hopkins P. F., Hernquist L., Cox T. J., Di Matteo T., Martini P., Robertson B., Springel V., 2005, ApJ, 630, 705
Hosokawa T., 2002, ApJ, 576, 75
Ivison R. J., Smail I., Papadopoulos P. P., Wold I., Richard J., Swinbank A. M., Kneib J., Owen F. N., 2010, MNRAS, 404, 198
Ivison R. J., Papadopoulos P. P., Smail I., Greve T. R., Thomson A. P., Xilouris E. M., Chapman S. C., 2011, MNRAS, 412, 1913
Ivison R. J. et al., 2012, MNRAS, 425, 1320
Jarvis M. J., McLure R. J., 2006, MNRAS, 369, 182
Kennicutt R. C., 1998, ARA&A, 36, 189
Lapi A., Shankar F., Mao J., Granato G. L., Silva L., De Zotti G., Danese L., 2006, ApJ, 650, 42
Magorrian J. et al., 1998, AJ, 115, 2285
Martini P., Weinberg D. H., 2001, ApJ, 547, 12
Omont A., McMahon R. G., Cox P., Kreysa E., Bergeron J., Pajot F., Storrie-Lombardi L. J., 1996, A&A, 315, 1
Page M. J., Stevens J. A., Ivison R. J., Carrera F. J., 2004, ApJ, 611, L85
Page M. J., Carrera F. J., Stevens J. A., Ebrero J., Blustin A. J., 2011, MNRAS, 416, 2792
Page M. J. et al., 2012, Nat, 485, 213
Papadopoulos P. P., Kovacs A., Evans A. S., Barthel P., 2008, A&A, 491, 483
Pascale E. et al., 2011, MNRAS, 415, 911
Pilbratt G. L. et al., 2010, A&A, 518, L1
Riechers D. A., 2011, ApJ, 730, 108
Riechers D. A. et al., 2011, ApJ, 739, L32
Sanders D. B., Soifer B. T., Elias J. H., Neugebauer G., Matthews K., 1988, ApJ, 328, L35
Schneider D. P. et al., 2010, AJ, 139, 2360
Schumacher H., Martínez-Sansigre A., Lacy M., Rawlings S., Schinnerer E., 2012, MNRAS, 423, 2132
Shaver P. A., 1988, in Osmer P., Phillips M. M., Green R., Foltz C., eds, ASP Conf. Ser. Vol. 2, Optical Surveys for Quasars. Astron. Soc. Pac., San Francisco, p. 265
Solomon P. M., Vanden Bout P. A., 2005, ARA&A, 43, 677
Solomon P. M., Downes D., Radford S. J. E., Barrett J. W., 1997, ApJ, 478, 144
Spergel D. N. et al., 2003, ApJS, 148, 175
Steidel C. C., Erb D. K., Shapley A. E., Pettini M., Reddy N., Bogosavljević M., Rudie G. C., Rakic O., 2010, ApJ, 717, 289

Stevens J. A., Page M. J., Ivison R. J., Carrera F. J., Mittaz J. P. D., Smail I., McHardy I. M., 2005, MNRAS, 360, 610
Swinbank A. M., Chapman S. C., Smail I., Lindner C., Borys C., Blain A. W., Ivison R. J., Lewis G. F., 2006, MNRAS, 371, 465
Swinbank A. M. et al., 2010, MNRAS, 405, 234
Swinbank A. M. et al., 2011, ApJ, 742, 11
Tacconi L. J., Genzel R., Lutz D., Rigopoulou D., Baker A. J., Iserlohe C., Tecza M., 2002, ApJ, 580, 73
Tacconi L. J. et al., 2006, ApJ, 640, 228
Tacconi L. J. et al., 2008, ApJ, 680, 246
Veilleux S. et al., 2009, ApJS, 182, 628
Vestergaard M., Peterson B. M., 2006, ApJ, 641, 689
Wandel A., 1999, ApJ, 527, 649
Wardlow J. L. et al., 2011, MNRAS, 415, 1479

This paper has been typeset from a TEX/LATEX file prepared by the author.